

# Computer Modeling and Weight Limit Analysis for Bridge Structure Fatigue Using OpenSEES

Lu Deng, Ph.D., M.ASCE<sup>1</sup>; Wangchen Yan<sup>2</sup>; and Shaofan Li, Ph.D.<sup>3</sup>

**Abstract:** With the increasing demand in freight transportation, truck overloading has become a common issue worldwide. Overloaded trucks pose great challenges for transportation administration in that they can jeopardize the safety of bridges and even lead to bridge collapse. Traditionally, vehicle-induced damage on bridges was estimated based on the line-girder analysis, as suggested by bridge design codes. These analysis methods have been criticized to overly underestimate the bridge capacity. In this study, the fatigue damage (FD) of a typical composite girder bridge under truck overloading was investigated using the OpenSEES framework. The bridge system was regarded as a series-parallel system composed of concrete deck slab and a steel girder subsystem. A method for determining rational vehicle weight limits for highway bridges to achieve the desired service life was proposed considering the FD of bridges. The proposed method could also be used for estimating the FD of bridges caused by truck overloading. Numerical simulation results obtained from this study have shown that the cumulative FD of bridges under severe overloading conditions could increase rapidly, and it may threaten the safety of bridges, which underscores the importance of enforcing truck weight regulations on highway bridges. DOI: [10.1061/\(ASCE\)BE.1943-5592.0001459](https://doi.org/10.1061/(ASCE)BE.1943-5592.0001459). © 2019 American Society of Civil Engineers.

**Author keywords:** Weight limit method; Fatigue analysis; System redundancy; OpenSEES; Composite bridges.

## Introduction

Because of the increasing demand for freight transportation, truck overloading has become a common issue worldwide and a big challenge for transportation administration. Overloaded trucks can lead to an accelerated deterioration of bridge components and can even cause bridges to collapse. Although truck overloading may not directly threaten the safety of new bridges, it poses a serious threat to the safety of old bridges (Mohammadi and Polepeddi 2000). Moreover, approximately 40% of bridges in the US are older than 50 years and over 9% of the bridges are considered structurally deficient according to the ASCE (2017) report card. Therefore, it is necessary to set rational truck weight limits to ensure the safety of existing bridges.

Bridge design codes, such as the AASHTO LRFD (AASHTO 2017) code, typically estimated the behavior of bridges using the linear-elastic analysis methods while treating the bridge as a one-dimensional (1D) line girder. These methods assume that the failure of a representative girder will lead to the failure of the entire bridge system (Gheitsi and Harris 2014, 2016; Sofi and Steelman 2017). However, some researchers criticized the idea that treating a bridge as a nonredundant system could overly underestimate the capacity

of the bridge system (Yang et al. 2004; Gheitsi and Harris 2014; Sofi and Steelman 2017). In addition, the deck slab and secondary elements could significantly increase the load-carrying capacity of the bridge system (Wood et al. 2007). Nevertheless, the fatigue design of the deck slab is not required in most bridge design codes (Yang et al. 2017), such as the AASHTO LRFD (AASHTO 2017) code. More importantly, there is still a lack of methods to evaluate the damage of structure systems (AASHTO 2018; Gheitsi and Harris 2016).

The objective of this study is to propose a rational weight limit method for bridges to achieve the desired service life based on the consideration of fatigue damage (FD). For this purpose, a typical steel-concrete composite bridge, which is one of the most popular bridge types in the US according to the National Bridge Inventory (NBI 2015), was selected to investigate the performance of a bridge system under overloading conditions. The open-source finite-element (FE) analysis tool, namely, the OpenSEES framework, was adopted in the structural analysis. According to Sofi and Steelman (2017), the system behavior of a bridge can be evaluated by analyzing the performance of the superstructure. In this study, the bridge superstructure was considered as a series-parallel system consisting of the bridge deck slab and the steel girder parallel subsystem. The FD of the superstructure system under truck overloading was investigated.

## Utilization of OpenSEES

FE analysis for bridges is typically conducted using commercial software packages, such as ANSYS, Abaqus, ADINA, and so forth. However, commercial software is usually not affordable to the public. In this study, an open-source FE analysis framework OpenSEES was adopted. The OpenSEES framework was originally developed for simulating the responses of structural and geotechnical systems subjected to earthquakes. In addition to the applications in seismic studies (Kashani et al. 2015; Jung and Andrawes 2018; Bosco and Tirca 2017), the OpenSEES

<sup>1</sup>Professor, Key Laboratory for Wind and Bridge Engineering of Hunan Province, College of Civil Engineering, Hunan Univ., Changsha, Hunan 410082, China. Email: denglu@hnu.edu.cn

<sup>2</sup>Ph.D. Candidate, College of Civil Engineering, Hunan Univ., Changsha, Hunan 410082, China; Dept. of Civil and Environmental Engineering, Univ. of California, Berkeley, CA 94720. Email: ywchener@berkeley.edu

<sup>3</sup>Professor, Dept. of Civil and Environmental Engineering, Univ. of California, Berkeley, CA 94720 (corresponding author). ORCID: <https://orcid.org/0000-0002-6950-1474>. Email: shaofan@berkeley.edu

Note. This manuscript was submitted on August 7, 2018; approved on March 27, 2019; published online on May 20, 2019. Discussion period open until October 20, 2019; separate discussions must be submitted for individual papers. This paper is part of the *Journal of Bridge Engineering*, © ASCE, ISSN 1084-0702.

**Table 1.** Basic information of the considered bridge

Component	Parameter	Value
Girder	Girder height (m)	1.61
	Cross-sectional area (m <sup>2</sup> )	0.02
	Moment of inertia (m <sup>4</sup> )	0.0011
	Young's modulus (GPa)	210
	Poisson's ratio	0.25
Deck	Deck thickness (m)	0.2
	Roadway width (m)	9.75
	Young's modulus (GPa)	33.5
	Poisson's ratio	0.167

framework has also been applied to other areas, such as load rating of bridge girders (Scott et al. 2008) and simulation of structural responses under fire (Jiang and Usmani 2013), showing good potential in the field of civil engineering. In this study, the OpenSEES framework was extended to the FD analysis of bridges under the action of truck overloading.

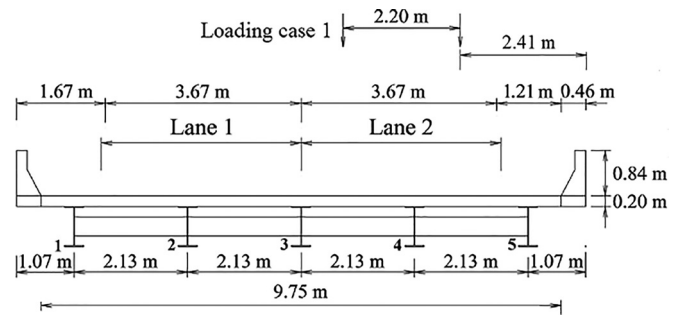
### Bridge Model

According to the report by Bae and Oliva (2010), the multi-girder bridge, especially the steel-concrete composite girder bridge (NBI 2015), is the most common type of bridge in the United States. In this study, a typical composite girder bridge with steel girders and concrete deck slab was selected to investigate the bridge FD under overloading conditions. This bridge model is a good representative of the simply supported steel-concrete composite girder bridges in the United States and has been widely used to investigate the behavior of bridges of this type (Wang et al. 2005, 2016; Deng et al. 2019). The bridge was designed according to the HS 20-44 truck load specified in the AASHTO LRFD (AASHTO 2017) code. It has a single span of 30.48 m and a deck slab of 10.67 m in width. This bridge has five identical steel I-girders with a space of 2.13 m in the transverse direction and five steel diaphragms evenly spaced at 7.62 m in the longitudinal direction. Some basic size information and material properties are listed in Table 1. The cross section of the bridge is illustrated in Fig. 1.

A three-dimensional (3D) FE model for this bridge was built using the OpenSEES framework. The concrete deck, steel girders, and guardrails were modeled by a standard brick element with eight nodes. The steel diaphragms were modeled by the ShellMITC4 element, which uses a bilinear isoparametric formulation together with a modified shear interpolation to improve the bending behavior of thin plates. It has been demonstrated that the asphalt pavement and the dead weight of other components, such as the waterproof layer and drainage facilities, have a negligible influence on the behavior of the superstructure and were therefore not considered in this study (Deng and Cai 2010; Yan et al. 2016). In addition, the mass of each girder was uniformly distributed along the longitudinal direction of the bridge. Because the OpenSEES framework does not offer pre-processing and postprocessing visualization modules, the model visualization and code check rely on other preprocessors and post-processors, such as the GiD software. In this study, the bridge model developed in the OpenSEES framework is illustrated by using the GiD software, as given in Fig. 2.

### Overloading Conditions

In this study, the HS 20-44 design fatigue truck with a gross weight of 320 kN, as given in Fig. 3, was adopted to investigate the vehicle-induced FD. This truck model was developed based on the

**Fig. 1.** Cross section of the selected composite bridge.

collected data of axle weights and spacings of a large number of four- and five-axle trucks, which make the largest contribution to the traffic-induced bridge FD (Schilling and Klippstein 1978; Schilling 1984). The axle weights ( $W_A$ ) of the first, second, and third axles of the design fatigue truck are 35.84, 142.08, and 142.08 kN, respectively.

Along with the design fatigue truck, four overloaded trucks with the same configuration as the HS 20-44 design fatigue truck were selected to study the effect of truck overloading. According to Siekmann et al. (2011), axle-weight-based overloading is more likely to take place than gross-weight-based overloading. Therefore, the axle-weight-based overloading strategy was adopted in this study and four trucks with axle weights of 1.25, 1.50, 1.75, and 2.00 times the axle weights of the design fatigue truck, respectively, were considered. Because the two traffic lanes of the bridge considered are symmetric about the central axis and the possibility of multiple vehicles traveling in the same lane is small (Nowak et al. 1993), only the scenario of one truck traveling along the centerline of the slow lane, as suggested by the AASHTO LRFD (AASHTO 2017) code, was investigated in this study. This scenario is illustrated by Loading case 1, as given in Fig. 1.

### Fatigue Analysis of the Bridge Structure

It was reported that vehicle-induced damage typically took place in the deck slab and other main superstructure members (Wang et al. 2005). Moreover, according to Sofi and Steelman (2017), the system behavior of the bridge structure can be represented by the behavior of the superstructure system. Therefore, only the superstructure, i.e., the concrete deck slab and the steel girders, was selected for the fatigue analysis in this study. Furthermore, the superstructure was considered as a series-parallel system (Estes and Frangopol 1999) in which the girders were regarded as a parallel subsystem connecting with the deck slab in series (Czarnecki and Nowak 2008; Yang et al. 2004). In the following, the failure of the bridge system induced by the failure of the deck slab and the failure of the girder subsystem was studied. The cumulative FDs of the concrete deck slab and steel girders were calculated based on the Miner's rule [Eq. (1)]. The Miner's rule was suggested for FD calculation by the AASHTO LRFD (AASHTO 2017) code and has been widely adopted in bridge design practices (Fatemi and Yang 1998; Guo and Chen 2013)

$$\text{Cumulative FD}(t) = \sum_i \frac{n_i}{N_i} \quad (1)$$

where  $n_i$  and  $N_i$  = number of the stress cycles experienced by the steel component and the number of stress cycles for the steel component to fail at the stress-range level  $S_i$ , respectively. In addition,

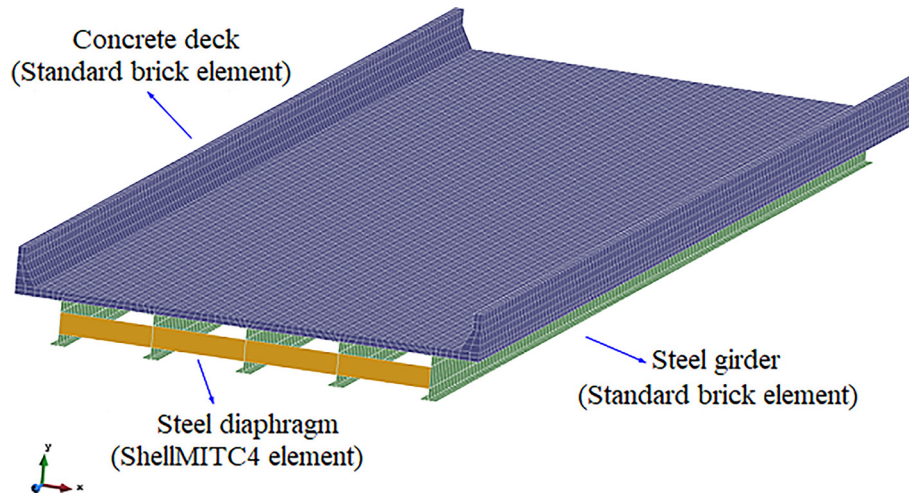


**Fig. 2.** Bridge model developed using the OpenSEES framework.

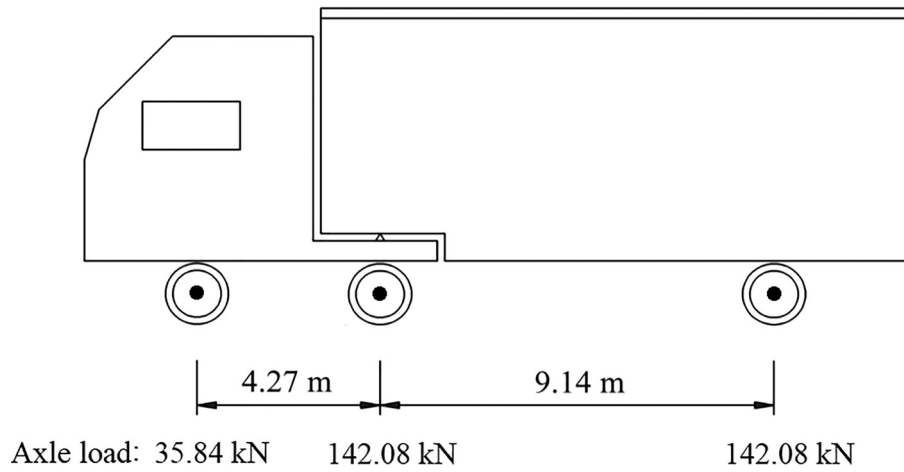


**Fig. 3.** Fatigue truck adopted.

the stress cycles were counted using the rainflow counting algorithm (Downing and Socie 1982).

### Fatigue Analysis for the Steel Girder Subsystem

In this study, the FD of each steel girder was estimated based on the longitudinal bending moment at midspan. According to the AASHTO LRFD code (AASHTO 2017), the stress range and the number of the stress cycles for the steel components hold the following relationship:

$$N_i = \frac{A}{S_i^m} \quad (2)$$

where  $m$  = slope constant of the  $S$ - $N$  curve; and  $A$  = fatigue constant. For the fatigue details considered in this study, namely, the welds connecting the bottom flange and the web of the steel girders,  $m$  can be taken as 3 approximately (Guo et al. 2012). For the flange and the web of the steel girders,  $A$  can be taken as  $3.93 \times 10^{12}$  MPa according to the AASHTO LRFD (AASHTO 2017) code.

According to the findings by Schilling (1984), vehicle-induced cumulative FD can be calculated from the maximum

stress range (MSR) and the equivalent number of stress cycles (ENSC). The MSR is defined as the algebraic difference between the maximum stress and the minimum stress. According to Connor et al. (2005) and Kwon et al. (2012), the stress ranges between 3.45 MPa and 33% of the constant amplitude fatigue limit (CAFL) were selected to count the effective stress cycles. In addition, the ENSC can be calculated using the following equation (Schilling 1984):

$$\text{ENSC} = \text{num} + \left(\frac{S_{r1}}{S_{rp}}\right)^m + \left(\frac{S_{r2}}{S_{rp}}\right)^m + \dots + \left(\frac{S_{ri}}{S_{rp}}\right)^m \quad (3)$$

where  $S_{rp}$  = primary stress range of the steel girder under consideration; num = number of primary stress cycles caused by an individual truck passage; and  $S_{ri}$  = higher order stress ranges.

Finally, the cumulative FD caused by passing trucks during a certain period can be determined by the following expression:

$$\text{Cumulative FD}(t) = \text{Num} \cdot \frac{\text{ENSC} \cdot \text{MSR}^3}{A} \quad (4)$$

where Num = number of trucks passing through the bridge during a certain period of time.

## Fatigue Analysis of the Concrete Deck Slab

The deck slab is directly subjected to traffic loading and may experience over 100 million loading cycles during the bridge's service life (Schläfli and Brühwiler 1998). However, the fatigue design of deck slabs was usually not considered in bridge design codes (Yang et al. 2017; AASHTO 2017). In this study, the FD of the concrete deck slab was investigated via the maximum transverse bending moment at midspan because the transverse bending moment is usually the controlling internal force of the bridge deck slab (Yu et al. 2017). Although the deterioration rate of the bridge deck slab varies between different locations and varies with time, it was assumed that the deterioration of the entire deck slab is uniform to avoid making the problem too complex. The same assumption was also adopted in other studies (Kostem 1982).

In the following, the calculation procedure for the FD of the concrete deck slab was derived in a manner similar to that of steel girders, which is helpful for the fatigue analysis of the bridge system. Based on a review of the  $S$ - $N$  curves for concrete components, the  $S$ - $N$  curve originally proposed by Aas-Jakobsen and Lenschow (1973) and modified by Tefers and Kutti (1979), as given in Eq. (5), was adopted in this study

$$\frac{S_{\max}}{S_{ck}} = 1 - \beta \cdot \left(1 - \frac{S_{\min}}{S_{\max}}\right) \cdot \log N' \quad (5)$$

where  $S_{ck}$  = concrete strength;  $S_{\max}$  and  $S_{\min}$  = maximum and minimum stresses, respectively;  $\beta$  is approximately 0.685 according to Tefers and Kutti (1979); and  $N'$  = number of cycles required for the concrete component to fail at a certain stress level. Then,  $S_{ck}$  was taken as 35 N/mm<sup>2</sup> for compression and 1.57 N/mm<sup>2</sup> for tension in this study.

With simple transformation, Eq. (5) can be rewritten as follows:

$$\frac{S_{\max} \left(1 - \frac{S_{\max}}{S_{ck}}\right)}{\beta (S_{\max} - S_{\min})} = \log N' \quad (6)$$

According to the definition of stress range  $S'_i$  as listed in Eq. (7), Eq. (6) can be expressed by Eq. (8).

$$S'_i = S_{\max} - S_{\min} \quad (7)$$

$$\frac{S_{\max} \left(1 - \frac{S_{\max}}{S_{ck}}\right)}{\beta \cdot S'_i} = \log N'_i \quad (8)$$

Because the parameters  $S_{\max}$ ,  $S_{ck}$ , and  $\beta$  are all constants, as mentioned previously, the term  $S_{\max}(1 - S_{\max}/S_{ck})/\beta$  is a constant and was assumed as the fatigue constant  $A'$  for the concrete deck slab. Then the relationship between the stress range and the loading cycle for the concrete deck slab, i.e., Eq. (8), can be expressed in a manner similar to that for steel girders, as shown in the following:

$$\frac{A'}{S'_i} = \log N'_i \quad (9)$$

According to Eq. (9), the cumulative FD (Cumulative FD'<sub>*i*</sub>) caused by an individual truck passage can be calculated as follows:

$$\text{Cumulative FD}'_i = \frac{n'_i}{N'_i} = \frac{n_i}{10^{A'/S'_i}} \quad (10)$$

Based on the equivalent FD concept (Oh 1991), it is expected that an equivalent number of stress cycles (ENSC') can be found for the maximum stress range (MSR') for concrete components. The cumulative FD of the concrete deck slab can be expressed by Eq. (11), which is similar to that of steel girders, as shown in Eq. (4)

$$\text{Cumulative FD}'(t) = \text{Num} \cdot \sum_{i=1}^n \frac{n'_i}{10^{A'/S'_i}} = \text{Num} \cdot \frac{\text{ENSC}'}{10^{A'/\text{MSR}'}} \quad (11)$$

where MSR' = maximum stress range for the concrete deck slab; and ENSC' can be determined from the following equation:

$$\begin{aligned} \text{ENSC}' &= \text{num}' + 10^{\frac{A'}{S'_{rp}} - \frac{A'}{S'_{r1}}} + 10^{\frac{A'}{S'_{rp}} - \frac{A'}{S'_{r2}}} + \dots + 10^{\frac{A'}{S'_{rp}} - \frac{A'}{S'_{ri}}} \\ &= \text{num}' + 10^{A' \cdot \left(\frac{1}{S'_{rp}} - \frac{1}{S'_{r1}}\right)} + 10^{A' \cdot \left(\frac{1}{S'_{rp}} - \frac{1}{S'_{r2}}\right)} + \dots \\ &\quad + 10^{A' \cdot \left(\frac{1}{S'_{rp}} - \frac{1}{S'_{ri}}\right)} \end{aligned} \quad (12)$$

where  $S'_{rp}$  = primary stress range for the concrete deck slab; and num' = number of primary stress cycles caused by each truck passage.

## Failure Analysis of the Bridge System

Based on the bridge model developed with the OpenSEES framework, the static analysis of the bridge was performed under Loading case 1, as given in Fig. 1. In the numerical simulations, the truck was set to travel through the bridge step by step with a step length of 0.2 m. The static transverse stress of concrete deck slab at midspan and the static longitudinal stress of the steel girder at midspan at each loading step were recorded. Then the dynamic load allowance specified in the AASHTO LRFD code (AASHTO 2017) was added to the static stress range to take the dynamic load effect into account when calculating the cumulative FD on the girders and deck slab.

In this study, the bridge system was represented by a series-parallel system that would fail if the failure of the deck slab or the failure of the girder subsystem occurred. Because the bridge is symmetric about the central axis, the failure of one lane could be deemed as the failure of the entire bridge system. For the loading case adopted in this study, as given in Fig. 1, the girders under Lane 2, namely, Girders 3–5, bear most of the vehicle load. The failure of any two adjacent girders of these three girders could lead to the failure of Lane 2 and therefore the failure of the bridge system. Similar assumptions were made in other studies (Estes and Frangopol 1999).

To determine the most vulnerable girder in the entire structure of the girder subsystem, the behavior of each girder was investigated after being subjected to the overloaded trucks with different weights, as given in Fig. 4. Fig. 4 demonstrates that the FD of each girder under the same loading is different, and the FD of Girder 5 is always the maximum because it experiences the largest stress among all the girders under the loading conditions considered. Therefore, Girder 5 is expected to fail first, followed by Girder 4, and then the other girders. Therefore, the failure of the two adjacent girders, i.e., Girders 5 and 4, can be regarded as the failure of the bridge system in this study.

Figs. 5(a and b) are the flowcharts for determining the failure of the bridge system, in which the girder subsystem was represented by an individual girder and any two adjacent girders, respectively.

In these flowcharts, “M-slab” denotes that the fatigue failure is caused by the bending moment of the deck slab, whereas “M-Girder 5” denotes that the fatigue failure is caused by the bending moment of Girder 5. Previous studies have shown that shear failure is not the controlling failure mode for this type of bridge (Brühwiler and Herwig 2008; González et al. 2011), therefore, it

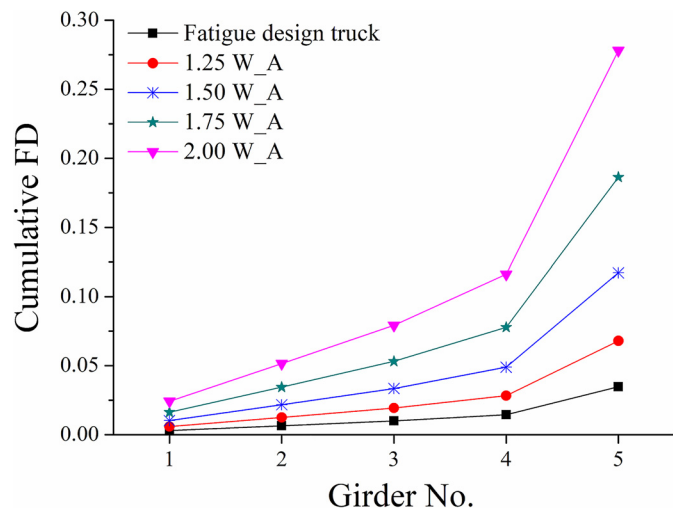


**Fig. 4.** Cumulative FD of each girder under different loading conditions.

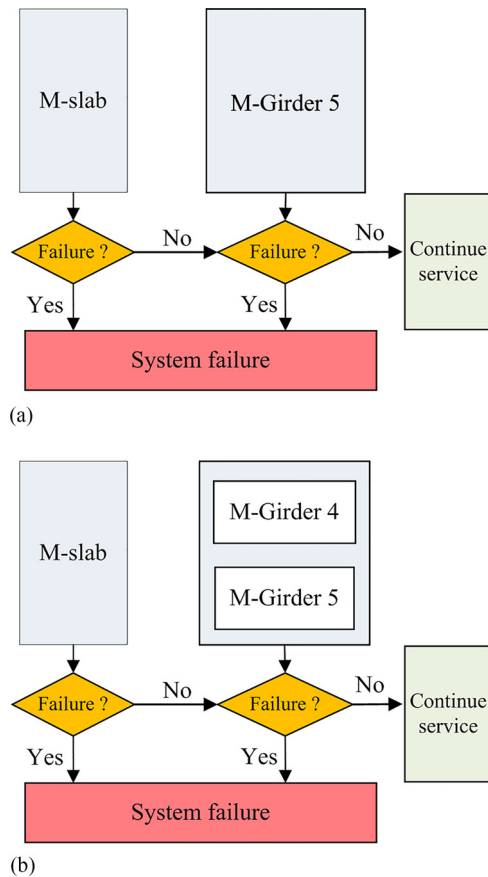


**Fig. 5.** Flowchart for bridge system failure: (a) girder subsystem represented by a single girder; and (b) girder subsystem represented by two adjacent girders.

is not considered in this study. In the following, the behavior of the girder subsystem represented by one girder and two adjacent girders was investigated.

### FD of the Bridge System

As discussed previously, the analysis of the bridge system in this study is focused on the performance of the superstructure, which was considered as a series-parallel structure system. Specifically, the girder subsystem was regarded as a parallel subsystem, and it is connected to the deck slab in series. In the following, we investigated the fatigue failure of the deck slab and the fatigue failure of the girder subsystem in detail.

### Cumulative FD of the Girder Subsystem

In the current design practices, multigirder bridges are usually designed based on the 1D line girder analysis methods (AASHTO 2017; Wood et al. 2007; Harris and Gheitsi 2013). In the following, the fatigue problem of Girder 5 was investigated according to the flowchart given in Fig. 5(a) and the results are given in Fig. 6.

Fig. 6 demonstrates that the FD of Girder 5 increases as the bridge service time increases. In addition, it is found that the cumulative FD increases more rapidly than the increase of the axle weight. Furthermore, it takes 75, 43, 27, and 18 years for the cumulative FD of Girder 5 to reach 1.0 under the loading of trucks with 1.25, 1.50, 1.75, and 2.00 W\_A, respectively. This nonlinear relationship between the fatigue life and axle weight ratio occurs because the FD is proportional to the third power of the stress that is linearly related to the axle weight.

Interestingly, the cumulative FD of Girder 5 under the loading of the truck with 1.25 W\_A reaches about 1.0 at the end of the design fatigue life of 75 years. In other words, the allowable overloading ratio considering the FD is roughly 25% in this study. Nevertheless, the overloading ratio corresponding to the weight cap of 363 kN by Bridge formula B was calculated to be 13%, which is smaller than the allowable ratio (25%) obtained from this study. In fact, the cap of 363 kN was criticized to be too arbitrary (Moshiri and Montufar 2016). This phenomenon indicates that bridges may be capable of carrying more loads than that allowed by Bridge formula B. Similar conclusions were found in other studies (Committee for the Truck Weight Study 1990; Moshiri and Montufar 2016; Deng and Yan 2018).

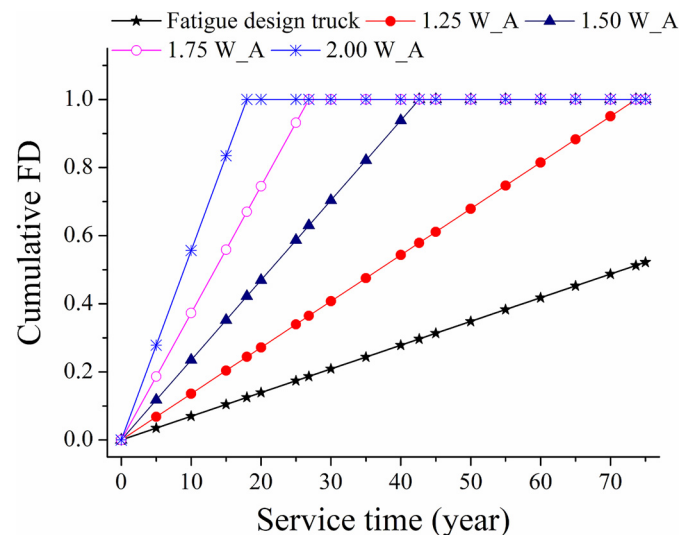


**Fig. 6.** Cumulative FD of Girder 5 under truck loading.

More importantly, the approximate overloading ratio of 25% in this study was obtained based on the behavior of a single representative girder in accordance with the AASHTO LRFD design method. It has been demonstrated that the analysis based on the component's behavior could underestimate the actual system behavior (Gheitsi and Harris 2014). Therefore, the approximate overloading ratio of 25% may be conservative. Furthermore, Eamon and Nowak (2002) pointed out that the collapse of the entire bridge is a more likely consequence than the failure of an individual girder. Consequently, the failure of the bridge girder subsystem based on the multigirder's behavior, as given in Fig. 5(b), was investigated in the following.

Generally, for the girder subsystem represented by a single girder, the girder with the maximum stress is the controlling component. In this study, Girder 5 is always the one with maximum longitudinal stress. Therefore, Girder 5 is the controlling girder when the girder subsystem is represented by an individual girder. However, this is not necessarily the case for the girder subsystem represented by multiple girders. In this study, when the girder subsystem is represented by multiple girders, two adjacent girders may be even more critical than a single girder, namely, Girder 5.

Note that in the single-girder-based approach, as suggested by the AASHTO LRFD (AASHTO 2017) code, each girder is designed according to the maximum load that it may possibly experience (Sofi and Steelman 2017). As a result, the girder may fail under the load effect that is larger than the design load effect, i.e., the maximum possible load effect. Furthermore, the maximum possible load effect can be calculated based on the 1D line-girder analysis with a proper girder distribution factor (GDF) (Harris and Gheitsi 2013; AASHTO 2017). According to the definition of the GDF, as shown in Eq. (13), the number of girders has no influence on the value of GDF. As a result, the maximum stress can be determined regardless of the number of girders. In the 3D FE analysis in this study, the design stress of the girder subsystem is regarded as the maximum possible stress that the girders may experience

$$\text{GDF} = 0.06 + \left(\frac{S}{14}\right)^{0.4} \left(\frac{S}{L}\right)^{0.3} \left(\frac{K_g}{12.0 L t_s^3}\right)^{0.1} \quad (13)$$

where  $S$  = girder spacing;  $L$  = span length;  $K_g$  = longitudinal stiffness parameter of the girder; and  $t_s$  = depth of concrete slab.

According to Fig. 5(b), the behavior of the girder subsystem represented by two adjacent girders (Girders 5 and 4) was analyzed in this study, and the results are given in Fig. 7. Unlike the constant deterioration rate for the girder subsystem represented by a single girder, the cumulative FD of the girder subsystem in Fig. 8 experiences two deterioration rates during the service life. The turning points are caused by the redistribution of the stress due to the failure of Girder 5. Additionally, the stress of Girder 4 after the failure of Girder 5 can be conservatively taken to be equivalent to the design stress, which was obtained from the 3D FE analysis.

Taking the girder subsystem under the overloading of truck with 1.75  $W_A$  in Fig. 7 as an example, the deterioration rate of the girder subsystem is controlled by the stress of Girder 4. According to Fig. 6, it takes 27 years for the FD of Girder 5 to reach 1.0 under the loading of truck with 1.75  $W_A$ . After that, the deterioration rate of the girder subsystem increases due to the increase of the stress of the controlling girder (Girder 4).

More importantly, under the same overloading condition, Fig. 7 and Fig. 6 demonstrate that the fatigue life of the subsystem represented by two adjacent girders (Fig. 7) is longer than that represented by a single girder (Fig. 6). This difference between the fatigue lives of the girder subsystem obtained based on the presence of multiple girders and each individual girder can be regarded as

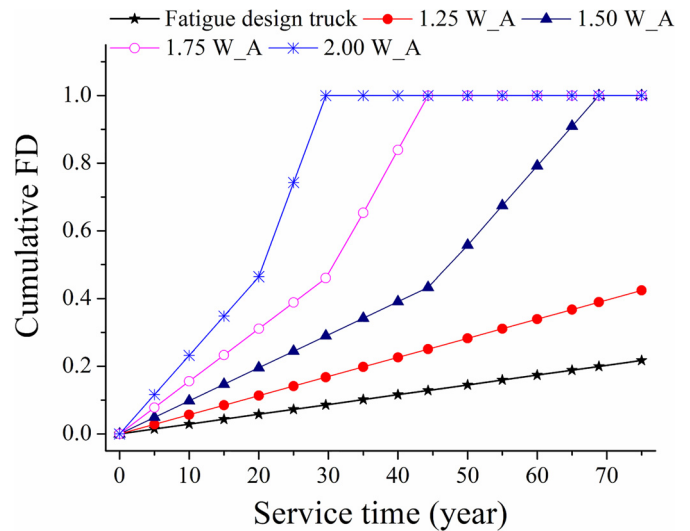


Fig. 7. Cumulative FD of the girder subsystem represented by two adjacent girders.

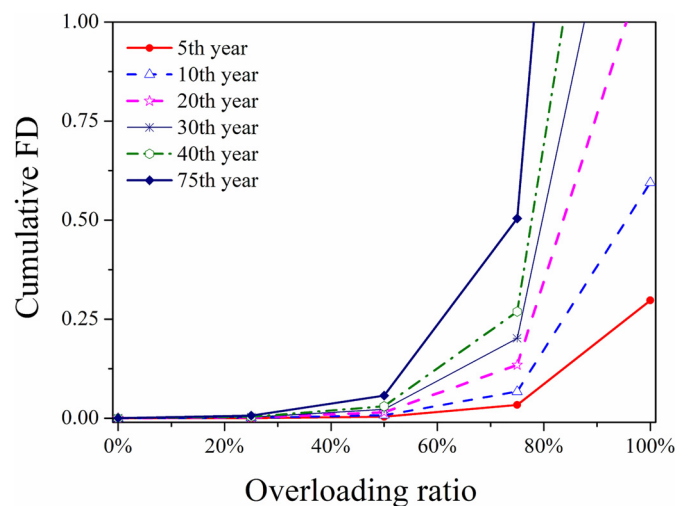


Fig. 8. Cumulative FD of the concrete deck slab under various overloading conditions.

an indication of the redundant level for the bridge (Estes and Frangopol 1999; Czarniecki and Nowak 2008).

Additionally, Fig. 6 clearly demonstrates that under the overloading of a truck with 1.25  $W_A$ , the cumulative FD of the girder subsystem based on the single girder behavior reaches 1.0 at the end of 75 years. In contrast, the cumulative FD of the girder subsystem based on the behavior of two adjacent girders reaches 0.42 at the end of 75 years, as given in Fig. 7, which is much less than 1.0. This difference can be attributed to the redundancy of the girder subsystem represented by multiple girders. Moreover, either based on the behavior of a single girder or that of multiple girders, the weight cap of 363 kN specified in Bridge formula B, which corresponds to an equivalent overloading ratio of 13%, seems to be too restrictive considering the FD.

#### Cumulative FD of the Deck Slab

In the superstructure system, the concrete deck slab is connected to multiple girders in series, as given in Figs. 4 and 6. The FD of the deck slab under various overloading conditions was calculated

according to Eq. (11), and the results are presented in Fig. 8. Fig. 8 demonstrates that under the loading of the HS 20-44 design fatigue truck, the cumulative FD of the deck slab at the end of the design service life is much less than 0.1 and can be neglected. However, under overloading conditions, the cumulative FD increases rapidly as the overloading ratio increases, especially when the overloading ratio exceeds 50%. Note that to make the curves clearer, not all FD results for the deck slab were plotted in Fig. 8.

Based on Fig. 8, the FD at the end of design service life for the deck slab under the loading of design fatigue trucks with 1.25, 1.50, and 1.75  $W_A$  is 0.0007, 0.0065, 0.0572, and 0.5045, respectively. This clearly shows that the FD increases exponentially as the load increases, as demonstrated by Eq. (11). As a result, truck overloading could cause rapid deterioration of both the concrete deck and the bridge system because the concrete deck was connected to the girder subsystem in serial.

### Weight Limit Analysis Considering the Cumulative FD of the Bridge System

In the following, the weight limit under which the bridge can achieve the desired service life was determined based on the FD of

both the deck slab and the girders. The method for calculating the cumulative FD was introduced in the previous section.

The single-girder-based approach assumes that the bridge system is a nonredundant system (Yang et al. 2004), although loads are shared by different bridge components (Czarnecki and Nowak 2008). This assumption could help the prediction of an early failure under truck overloading according to Fig. 6. However, this contradicts the fact that the collapse of the entire bridge is more realistic than the failure of an individual girder (Eamon and Nowak 2002). Therefore, it is not appropriate to set weight limits for the bridge based on the behavior of a single girder. In this study, the behavior of the girder subsystem represented by two adjacent girders has been investigated, and the procedure of determining the weight limit based on the behavior of bridge system is illustrated in Fig. 9.

Taking the composite steel girder bridge adopted in this study as an example, the weight limit method considering the system behavior is explained in the following. It is assumed that the cumulative FD of an existing bridge is 0.4 after 30 years of service, and the expected service life for the bridge is 75 years. According to Fig. 9, the detailed procedures for determining the vehicle weight limit are listed as follows.

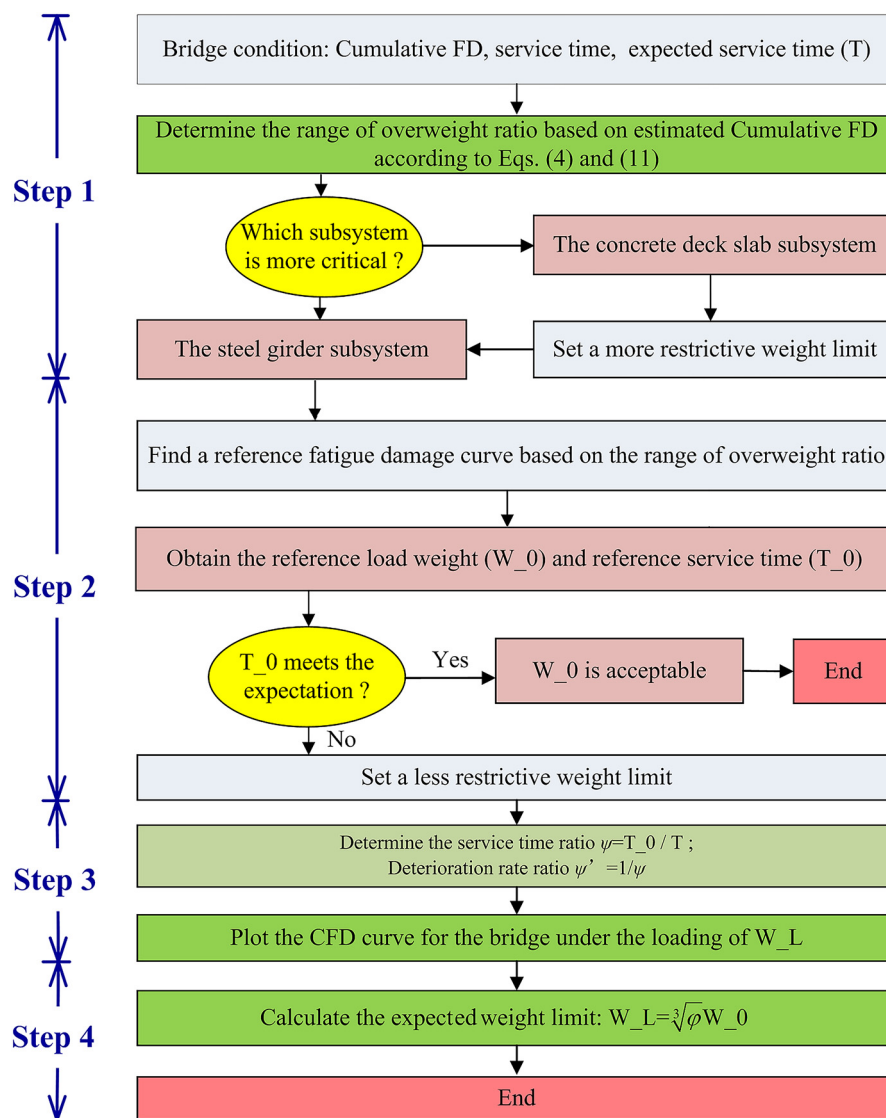


Fig. 9. Flowchart for determining the weight limit.

### Step 1: Determine Which Subsystem Is More Critical

The purpose of this step is for the deck slab to avoid being the critical subsystem under overloading conditions. Based on the current damage condition, it can be deduced from Fig. 8 that the cumulative FD of the concrete deck slab under the assumed loading condition increases rapidly and would reach around 0.75 at the end of expected service life, which is still less than 1.0. Therefore, the concrete deck slab is not the critical subsystem to determine the vehicle weight limit.

### Step 2: Determine the Reference Loading Level

According to the cumulative FD depicted in Fig. 7, the vehicle load should be within the range of 1.25–1.50  $W_A$  so that the cumulative FD could reach 1.0 at the end of 75 years. In this study, 1.50  $W_A$  was selected as the reference loading level, which corresponds to a total service life of 69 years and a remaining service life of 39 years, according to Fig. 7. Note that the total service life and the remaining service life were selected as the reference service time in this study. Unfortunately, neither of the reference service times meets the desired service life, namely, a total service time of 75 years and a remaining service time of 45 years.

To illustrate the detailed procedure and show the expected FD curves more clearly, the curves for the cumulative FD under the loading of trucks with 1.50 and 1.25  $W_A$  are depicted purposely in Fig. 10, and these two curves are defined as the reference FD curves.

### Step 3: Determine the Deterioration Rate Based on the Reference FD Curves

Even though the FD based on multiple girders' behaviors experiences two stages (Stages 1 and 2, as given in Fig. 10) with different accumulation rates, the ratio of the accumulation rates under different loading conditions is constant, as demonstrated by Eq. (4).

Specifically, the remaining service lives of the girder subsystem in Stages 1 and 2 under the loading of a truck with 1.50  $W_A$  are denoted as  $t_0$  and  $t_1$ , respectively, as presented in Fig. 10. Similarly, the remaining service lives of the girder subsystems under the expected weight limit ( $W_L$ ) are denoted as  $t'_0$  and  $t'_1$ , respectively. Then, the ratio of the remaining fatigue life under these two loading conditions can be calculated as

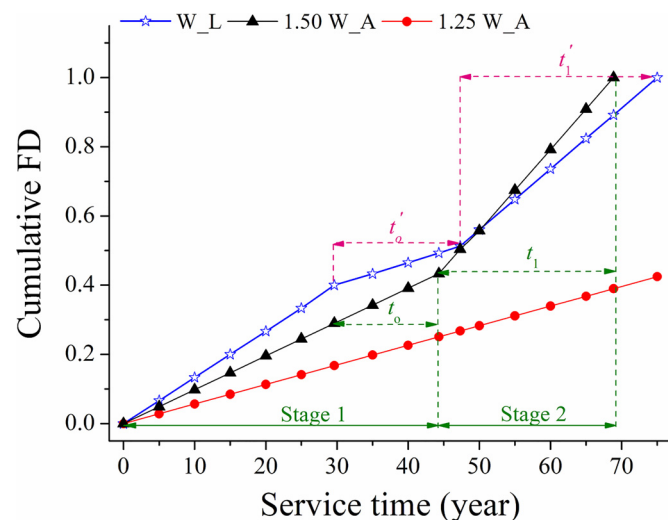


**Fig. 10.** Weight limit based on the cumulative FD of the bridge system.

$$\varphi = \frac{t_0}{t'_0} = \frac{t_1}{t'_1} = \frac{t_0 + t_1}{t'_0 + t'_1} = \frac{39}{45} = 0.867$$

Correspondingly, the ratio of the deterioration rate is  $\varphi' = 1/\varphi = 1.153$ , based on which the cumulative FD curve due to the loading of truck with expected weight can be depicted in Fig. 10.

### Step 4: Determine the Rational Weight Limit Based on the Remaining Life Ratio

According to Eq. (4), the expected weight limit can be obtained based on the remaining fatigue life ratio ( $\varphi$ ) and the reference loading level (1.50  $W_A$ ):  $W_L = \sqrt[3]{\varphi} \cdot 1.50 W_A = 1.43 W_A$ .

The proposed weight limit method could be used for determining the weight limit for existing bridges and for estimating the FD of bridges under truck overloading.

## Summary and Conclusions

In this study, the application of the OpenSEES framework was extended to the fatigue analysis of bridges. A typical steel-concrete composite girder bridge was adopted to investigate the FD under overloading conditions. The fatigue analysis of the bridge system focuses on the behavior of the superstructure, which was considered as a series-parallel system. Based on the fatigue analysis, a weight limit method was proposed considering the behavior of the bridge system under overloading. The proposed method can be applied to assist in determining the truck weight limit and to evaluate the FD of existing bridges under overloading conditions.

Based on the fatigue analysis of the bridge considered, the following conclusions can be drawn: (1) under severe overloading conditions, the cumulative FD could increase rapidly and may threaten the bridge safety; (2) the single-girder-based approach would predict an early failure of the bridge system under overloading conditions because the redundancy due to the system behavior of the bridge structure was overly simplified and underestimated, and (3) for the bridge considered in this study, the allowable overloading ratio was 25% if the single girder based approach is used, which is larger than the ratio of 13% corresponding to the gross weight cap of 363 kN specified in Bridge formula B. This cap value has been criticized to be too restrictive for overloaded trucks. These conclusions were based on the results from the bridge adopted in this study. To draw more general conclusions and to comment on the rationality of the truck weight regulations, more comprehensive analyses on a number of different types of bridges should be performed.

## Acknowledgments

The authors gratefully acknowledge the financial support provided by the National Natural Science Foundation of China (Grant 51778222), the China Scholarship Council (Grant 201706130087), and the Key Research Project of Hunan Province (Grant 2017SK2224).

## References

- AASHTO. 2017. *LRFD bridge design specifications*. 6th ed. Washington, DC: AASHTO.
- AASHTO. 2018. *The manual for bridge evaluation*. 3rd ed. Washington, DC: AASHTO.

- Aas-Jakobsen, K., and R. Lenschow. 1973. "Behavior of reinforced columns subjected to fatigue loadings." *ACI J.* 70 (3): 199–206.
- ASCE. 2017. "2017 Infrastructure Report Card." Accessed June 20, 2017. <https://www.infrastructurereportcard.org/cat-item/bridges/>.
- Bae, H., and M. G. Oliva. 2010. *Bridge analysis and evaluation of effects under overload vehicles*. Rep. No. CFIRE02-03. Madison, WI: Univ. of Wisconsin.
- Bosco, M., and L. Tirca. 2017. "Numerical simulation of steel I-shaped beams using a fiber-based damage accumulation model." *J. Constr. Steel Res.* 133 (Jun): 241–255. <https://doi.org/10.1016/j.jcsr.2017.02.020>.
- Brühwiler, E., and A. Herwig. 2008. "Consideration of dynamic traffic action effects on existing bridges at ultimate limit state." In *Proc., IABMAS'08: 4th Int. Conf. on Bridge Maintenance, Safety and Management*, edited by H. M. Koh and D. M. Frangopol, 3675–3682. London: Taylor & Francis.
- Committee for the Truck Weight Study. 1990. *Truck weight limits: Issues and options*. TRB Special Rep. 225. Washington, DC: Transportation Research Board, National Research Council.
- Connor, R., I. Hodgson, H. Mahmoud, and C. Bowman. 2005. *Field testing and fatigue evaluation of the I-79 Neville Island Bridge over the Ohio River*. Atlss Rep. No. 05-02. Bethlehem, PA: Lehigh Univ. Center for Advanced Technology for Large Structural Systems.
- Czarnecki, A. A., and A. S. Nowak. 2008. "Time-variant reliability profiles for steel girder bridges." *Struct. Saf.* 30 (1): 49–64. <https://doi.org/10.1016/j.strusafe.2006.05.002>.
- Deng, L., and C. Cai. 2010. "Bridge model updating using response surface method and genetic algorithm." *J. Bridge Eng.* 15 (5): 553–564. [https://doi.org/10.1061/\(ASCE\)BE.1943-5592.0000092](https://doi.org/10.1061/(ASCE)BE.1943-5592.0000092).
- Deng, L., and W. Yan. 2018. "Vehicle weight limits and overload permit checking considering the cumulative fatigue damage of bridges." *J. Bridge Eng.* 23 (7): 04018045. [https://doi.org/10.1061/\(ASCE\)BE.1943-5592.0001267](https://doi.org/10.1061/(ASCE)BE.1943-5592.0001267).
- Deng, L., W. Yan, and L. Nie. 2019. "A simple corrosion fatigue design method for bridges considering the coupled corrosion-overloading effect." *Eng. Struct.* 178 (Jan): 309–317. <https://doi.org/10.1016/j.engstruct.2018.10.028>.
- Downing, S. D., and D. F. Socie. 1982. "Simple rainflow counting algorithms." *Int. J. Fatigue* 4 (1): 31–40. [https://doi.org/10.1016/0142-1123\(82\)90018-4](https://doi.org/10.1016/0142-1123(82)90018-4).
- Eamon, C., and A. Nowak. 2002. "Effects of edge-stiffening elements and diaphragms on bridge resistance and load distribution." *J. Bridge Eng.* 7 (5): 258–266. [https://doi.org/10.1061/\(ASCE\)1084-0702\(2002\)7:5\(258\)](https://doi.org/10.1061/(ASCE)1084-0702(2002)7:5(258)).
- Estes, A., and D. Frangopol. 1999. "Repair optimization of highway bridges using system reliability approach." *J. Struct. Eng.* 125 (7): 766–775. [https://doi.org/10.1061/\(ASCE\)0733-9445\(1999\)125:7\(766\)](https://doi.org/10.1061/(ASCE)0733-9445(1999)125:7(766)).
- Fatemi, A., and L. Yang. 1998. "Cumulative fatigue damage and life prediction theories: A survey of the state of the art for homogeneous materials." *Int. J. Fatigue* 20 (1): 9–34. [https://doi.org/10.1016/S0142-1123\(97\)00081-9](https://doi.org/10.1016/S0142-1123(97)00081-9).
- Gheitsi, A., and D. Harris. 2014. "Failure characteristics and ultimate load-carrying capacity of redundant composite steel girder bridges: Case study." *J. Bridge Eng.* 20 (3): 05014012. [https://doi.org/10.1061/\(ASCE\)BE.1943-5592.0000667](https://doi.org/10.1061/(ASCE)BE.1943-5592.0000667).
- Gheitsi, A., and D. Harris. 2016. "Redundancy and operational safety of composite stringer bridges with deteriorated girders." *J. Perform. Constr. Facil.* 30 (2): 04015022. [https://doi.org/10.1061/\(ASCE\)CF.1943-5509.0000764](https://doi.org/10.1061/(ASCE)CF.1943-5509.0000764).
- González, A., D. Cantero, and E. J. OBrien. 2011. "Dynamic increment for shear force due to heavy vehicles crossing a highway bridge." *Comput. Struct.* 89 (23–24): 2261–2272. <https://doi.org/10.1016/j.compstruc.2011.08.009>.
- Guo, T., and Y. W. Chen. 2013. "Fatigue reliability analysis of steel bridge details based on field-monitored data and linear elastic fracture mechanics." *Struct. Infrastruct. Eng.* 9 (5): 496–505. <https://doi.org/10.1080/15732479.2011.568508>.
- Guo, T., D. M. Frangopol, and Y. Chen. 2012. "Fatigue reliability assessment of steel bridge details integrating weigh-in-motion data and probabilistic finite element analysis." *Comput. Struct.* 112–113 (Dec): 245–257. <https://doi.org/10.1016/j.compstruc.2012.09.002>.
- Harris, D. K., and A. Gheitsi. 2013. "Implementation of an energy-based stiffened plate formulation for lateral load distribution characteristics of girder-type bridges." *Eng. Struct.* 54 (Sep): 168–179. <https://doi.org/10.1016/j.engstruct.2013.04.002>.
- Jiang, J., and A. Usmani. 2013. "Modeling of steel frame structures in fire using OpenSees." *Comput. Struct.* 118 (Mar): 90–99. <https://doi.org/10.1016/j.compstruc.2012.07.013>.
- Jung, D., and B. Andrawes. 2018. "Seismic damage assessment of SMA-retrofitted multiple-frame bridge subjected to strong main shock–after-shock excitations." *J. Bridge Eng.* 23 (1): 04017113. [https://doi.org/10.1061/\(ASCE\)BE.1943-5592.0001164](https://doi.org/10.1061/(ASCE)BE.1943-5592.0001164).
- Kashani, M. M., L. N. Lowes, A. J. Crewe, and N. A. Alexander. 2015. "Phenomenological hysteretic model for corroded reinforcing bars including inelastic buckling and low-cycle fatigue degradation." *Comput. Struct.* 156 (Aug): 58–71. <https://doi.org/10.1016/j.compstruc.2015.04.005>.
- Kostem, C. N. 1982. *Further parametric studies on the overloading of highway bridges*. FHWA-PA-RD-77-2-1. Bethlehem, PA: Fritz Engineering Laboratory, Lehigh Univ.
- Kwon, K., D. Frangopol, and M. Soliman. 2012. "Probabilistic fatigue life estimation of steel bridges by using a bilinear S-N approach." *J. Bridge Eng.* 17 (1): 58–70. [https://doi.org/10.1061/\(ASCE\)BE.1943-5592.0000225](https://doi.org/10.1061/(ASCE)BE.1943-5592.0000225).
- Mohammadi, J., and R. Polepeddi. 2000. "Bridge rating with consideration for fatigue damage from overloads." *J. Bridge Eng.* 5 (3): 259–265. [https://doi.org/10.1061/\(ASCE\)1084-0702\(2000\)5:3\(259\)](https://doi.org/10.1061/(ASCE)1084-0702(2000)5:3(259)).
- Moshiri, M., and J. Montufar. 2016. "Existing bridge formulas for truck-weight regulation from international jurisdictions and resulting load stresses on single-span bridges." *J. Transp. Eng.* 142 (1): 04015038. [https://doi.org/10.1061/\(ASCE\)TE.1943-5436.0000810](https://doi.org/10.1061/(ASCE)TE.1943-5436.0000810).
- NBI (National Bridge Inventory). 2015. "Deficient bridges by superstructure material 2015." *Bridges and Structures*. Accessed December 31, 2015. <https://www.fhwa.dot.gov/bridge/nbi/no10/mat15.cfm>.
- Nowak, A., H. Nassif, and L. DeFrain. 1993. "Effect of truck loads on bridges." *J. Transp. Eng.* 119 (6): 853–867. [https://doi.org/10.1061/\(ASCE\)0733-947X\(1993\)119:6\(853\)](https://doi.org/10.1061/(ASCE)0733-947X(1993)119:6(853)).
- Oh, B. H. 1991. "Cumulative damage theory of concrete under variable-amplitude fatigue loadings." *Mater. J.* 88 (1): 41–48.
- Schilling, C. 1984. "Stress cycles for fatigue design of steel bridges." *J. Struct. Eng.* 110 (6): 1222–1234. [https://doi.org/10.1061/\(ASCE\)0733-9445\(1984\)110:6\(1222\)](https://doi.org/10.1061/(ASCE)0733-9445(1984)110:6(1222)).
- Schilling, C. G., and K. H. Klippstein. 1978. "New method for fatigue design of bridges." *J. Struct. Div.* 104 (3): 425–438.
- Schläfli, M., and E. Brühwiler. 1998. "Fatigue of existing reinforced concrete bridge deck slabs." *Eng. Struct.* 20 (11): 991–998. [https://doi.org/10.1016/S0141-0296\(97\)00194-6](https://doi.org/10.1016/S0141-0296(97)00194-6).
- Scott, M., A. Kidarsa, and C. Higgins. 2008. "Development of bridge rating applications using OpenSees and Tcl." *J. Comput. Civ. Eng.* 22 (4): 264–271. [https://doi.org/10.1061/\(ASCE\)0887-3801\(2008\)22:4\(264\)](https://doi.org/10.1061/(ASCE)0887-3801(2008)22:4(264)).
- Siekman, A., G. Capps, and M. B. L. Hudson. 2011. *Preliminary assessment of overweight mainline vehicles*. ORNL/TM-2011/463. Oak Ridge, TN: Oak Ridge National Laboratory.
- Sofi, F., and J. Steelman. 2017. "Parametric influence of bearing restraint on nonlinear flexural behavior and ultimate capacity of steel girder bridges." *J. Bridge Eng.* 22 (7): 04017033. [https://doi.org/10.1061/\(ASCE\)BE.1943-5592.0001065](https://doi.org/10.1061/(ASCE)BE.1943-5592.0001065).
- Tepfers, R., and T. Kutti. 1979. "Fatigue strength of plain ordinary and lightweight concrete." *ACI J.* 76 (5): 635–652.
- Wang, T., C. Liu, D. Huang, and M. Shahawy. 2005. "Truck loading and fatigue damage analysis for girder bridges based on weigh-in-motion data." *J. Bridge Eng.* 10 (1): 12–20. [https://doi.org/10.1061/\(ASCE\)1084-0702\(2005\)10:1\(12\)](https://doi.org/10.1061/(ASCE)1084-0702(2005)10:1(12)).
- Wang, W., L. Deng, and X. Shao. 2016. "Number of stress cycles for fatigue design of simply-supported steel I-girder bridges considering the dynamic effect of vehicle loading." *Eng. Struct.* 110 (Mar): 70–78. <https://doi.org/10.1016/j.engstruct.2015.11.054>.
- Wood, S., N. Akinci, J. Liu, and M. D. Bowman. 2007. *Long-term effects of super heavy-weight vehicles on bridges*. FHWA/IN/JTRP-2007/10. West Lafayette, IN: Purdue Univ.

- Yan, W., L. Deng, and X. Yin. 2016. "Allowable slope change of approach slabs based on the interacted vibration with passing vehicles." *KSCE J. Civ. Eng.* 20 (6): 2469–2482. <https://doi.org/10.1007/s12205-015-0466-1>.
- Yang, D. H., T. H. Yi, and N. H. Li. 2017. "Coupled fatigue-corrosion failure analysis and performance assessment of RC bridge deck slabs." *J. Bridge Eng.* 22 (10): 04017077. [https://doi.org/10.1061/\(ASCE\)BE.1943-5592.0001108](https://doi.org/10.1061/(ASCE)BE.1943-5592.0001108).
- Yang, S. I., D. M. Frangopol, and L. C. Neves. 2004. "Service life prediction of structural systems using lifetime functions with emphasis on bridges." *Reliab. Eng. Syst. Saf.* 86 (1): 39–51. <https://doi.org/10.1016/j.ress.2003.12.009>.
- Yu, Y., L. Deng, W. Wang, and C. S. Cai. 2017. "Local impact analysis for deck slabs of prestressed concrete box-girder bridges subject to vehicle loading." *J. Vib. Control* 23 (1): 31–45. <https://doi.org/10.1177/1077546315575434>.